ASM Sc. J., 13, Special Issue 1, 2020 for ICFICE, 75-81

Automatic Segmentation for Welding Defect Detection on Ceramics based on Fuzzy Clustering and Fuzzy Binarization

Kwang Baek Kim[1*] and Doo Heon Song[2]

[1]*Division of Computer Software Engineering, Silla University, Busan, Korea*

[2]*Department of Computer Games, Yong-In SongDam College, Yong-in, Korea*

Defects or cracks of ceramic materials produced in welding process can jeopardize the structural health of important constructs such as ship and airplane. Automatic segmentation of radiograph images is an essential component of the much-needed automatic defect inspection system in nondestructive testing of ship building industries. In this paper, we propose a method based on fuzzy logic in intensity enhancement and binarization. After anisotropic filtering, we apply fuzzy stretching to enhance the intensity contrast. Then we apply fuzzy binarization to form a defect object. In that process, we apply Fuzzy C-Means clustering to determine adaptive threshold parameter of the binarization. In experiment, the proposed method shows more stable and highly successful rate in defect detection from 80 welding radiographic images with 92.5% success rate compared with 53.8% of previous K-means based approach. Also, the proposed method can find defects from relatively thicker materials (including 16mm and 22mm) as well as thin material images which was regarded as a weak point of using radiographic image inspections.

Keywords: anisotropic filter; ceramic welding defect; fuzzy stretching; fuzzy c-means; fuzzy binarization

I. INTRODUCTION

Nondestructive Testing (NDT) refers to a group of analysis techniques to find defects and disorders of materials or a product without damaging its functional of shaping properties. In NDT of metallic pieces, the most important stage is the detection of welding defects which are detrimental to the final product quality (Thiruganam *et al*., 2010; Rajkolhe & Khan., 2014). Welding is used in many engineering applications such as ship construction (Kahanov *et al*., 2015; Suratkar *et al*., 2013; Zhang, 2016), automobile industries, bridge constructions, and aircraft machine frames constructions (Ma & Zhou., 2014). In welding of ship materials, there is a great discrepancy between theoretical and observed fracture strength due to the presence of very small, microscopic flaws and cracks that even happens under normal conditions (Zhang, 2016).

There are a number of nondestructive evaluation techniques available for producing two-dimensional and three-dimensional images of an object and X-ray imaging is widely used in industry since the experts are able to identify most types of defects in the images produced by this method. The method is based on the fact that the defective areas absorb more energy and thus the defects appear darker in the image. However, the interpretation of weld radiographs is subjective in that even experienced inspectors may disagree with each other and often time-consuming (Valavanis & Kosmopoulos, 2010). However, radiographic analysis is regarded as a weak method in detecting delicate but dangerous flaws especially in the thick sections (Marefat *et al*., 2011). Furthermore, there can be the inspector subjectivity (Kim & Woo, 2010).

Thus, it is natural to pursuit to build an automatic welding inspection system (Kim & Woo, 2010; Wang & Liao, 2002) to detect cracks, spiracles, and other foreign substances that form various types of defects to maintain the reliability of the

*Corresponding author's e-mail: gbkim@silla.ac.kr

metal constructs whether they are thin or thick.

Such automatic inspection system typically consists of three components such as image segmentation, feature extraction, and defect pattern classification. In the segmentation phase, it requires efficient noise removal and enhances the image contrast to detect the defects from the image so that the principal objects in the image can be more apparent than the background. Then, we need a meaningful set of features that characterizes welding defects with high discriminatory power. Various machine learning techniques are then applied to classify defect patterns using neural network (Valavanis & Kosmopoulos, 2010; Kesharaju *et al.*, 2014), fuzzy K-means (Zapata *et al.*, 2010), and C4.5 (Chen *et al.*, 2013).

However, segmentation step remains a very delicate process since there are many occasions having irregular types of noise and low contrasted images (Thiruganam *et al.*, 2010). From different perspective, adaptive edge detecting algorithms with contour analysis (Hocenski *et al.*, 2006; Mansoory *et al.*, 2008) have been used in defect detection but these techniques are argued due to its sensitivity to the noise (Silveria *et al.*, 2009). Automatic intelligent threshold supplements of this strategy (Mansoory *et al.*, 2008; Sarin *et al*, 2018) also suffer from the low brightness contrast of given images. Actually the defect detection in the segmentation step can be framed as a pixel clustering followed by an object forming process, where the goal is to classify each image pixel as a defect or not (Ferguson *et al.*, 2018; Kim & Song., 2016).

With object formation by pixel clustering strategy, K-means (Kim & Woo, 2014) and ART2 learning (Kim *et al.*, 2018) have been tried and obtain reasonable result. While being effective in most cases, both strategies need careful preprocessing for noise removal and image contrast enhancement. Also, ART2 learning was undesirably sensitive to the boundary variable values so that the scalability of such strategy was questioned (Kim & Song ., 2017). Several filtering and binarization combinations are applied to find optimal defect identification in ceramic materials but each strategy has pros and cons (Kim & Song., 2017; Kim *et al.*, 2014; Kim & Song, 2016).

In this paper, we try to optimize automatic segmentation process for welding ceramic materials. We adopt anisotropic filtering (Kim *et al.*, 2014) with fuzzy stretching for intensity contrast enhancement. Furthermore, fuzzy binarization algorithm is applied based on Fuzzy C-Means (FCM) clustering to decide adaptive threshold for the pixel classification. This new approach will be compared with K-means clustering based approach (Kim & Woo, 2014). The ceramic images tested in this paper have various thickness types such as 8mm, 10mm, 11mm, 16mm, and 22mm for ship building materials.

II. MATERIALS AND METHOD

A. Contrast enhancement

We adopt anisotropic filtering (Perona & Malik, 1990) to enhance the image quality since it can eliminate aliasing effects and reduce blurring compared with Gaussian filtering. It has been successful to enhance the quality of the original image for various applications such as satellite images (Grazzini *et al.*, 2005), astronomical images (Chao & Tsai ; 2006), medical images (Villain *et al.*, 2003), and forensic images (Meihua & Zhengming., 2004). However, this scheme alone is not sufficient to solve our goal of image contrast enhancement since it smoothies the information identically in all directions (Abdallah *et al.*, 2016). We use this filter only to enhance the general quality of input image. The filter is defined as equation (1).

$$I_t = div(c(x,y,t)\nabla I = c(x,y,t)\Delta I + \nabla c \cdot \nabla I \quad (1)$$

where div denotes divergence operator and $\bigtriangledown$ and Δ demote gradient and Laplacian operator respectively with conduction coefficient $c(x,y,t)$. The effect of anisotropic filtering is as shown in Figure 1.

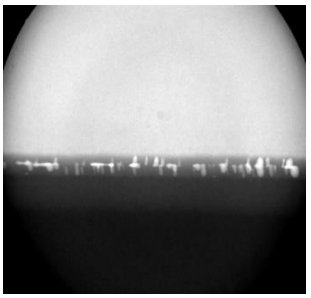

(a) Input Shape

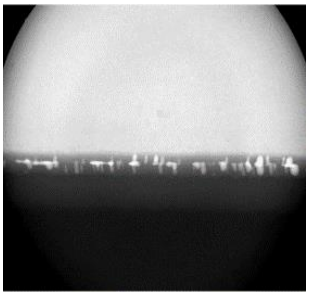

(b) After Filtering

Figure 1. The Effect of anisotropic filtering

From the ceramic X-ray image of ship building material, we

apply horizontal and vertical histogram and extract region of interest (ROI) for welding. Then, remove the background with least square method. The result might be as shown in Figure 2.

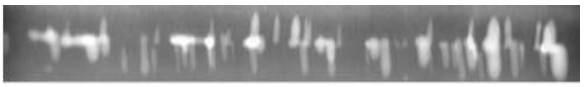

Figure 2. ROI after least square

In order to enhance the intensity contrast to identify the defect area, we apply fuzzy stretching with trapezoid type membership function. In general, fuzzy logic based intensity enhancement is more noise tolerant (Shin & Jung., 2017). Our fuzzy stretching process can be described as follows. The average intensity is as shown in equation (2).

$$X_m = \sum_{i=0}^{MN} \frac{X_i}{MN} \tag{2}$$

where Xi denotes the intensity value of current pixel and M, N denote the width and the height of the region respectively. The distance from the brightest pixel(D_{max}) and the darkest pixel(D_{min}) are defined as equation (3).

$$\begin{aligned} D_{min} &= |X_{max} - X_m| \\ D_{max} &= |X_m - X_{inm}| \end{aligned} \tag{3}$$

The adjustment rate (δ) is defined as equation (4).

$$\begin{aligned} &if(X_m > 128)\ then\ \delta = 255 - X_m \\ &else\ if(X_m \le D_{min})\ then\ \delta = D_{min} \\ &else\ if(X_m \ge D_{max})\ then\ \delta = D_{max} \\ &else\ \delta = X_m \end{aligned} \tag{4}$$

Then the membership function of our fuzzy stretching is shown as Figure 3 and important interval points of the membership function are defined as equation (5).

$$\begin{aligned} I_{max} &= X_m + \delta \\ I_{min} &= X_m - \delta \\ I_{mid} &= (I_{max} + I_{min})/2 \\ I_{mid1} &= (I_{mid} + I_{min})/2 \\ I_{mid2} &= (I_{mid} + I_{max})/2 \end{aligned} \tag{5}$$

There are critical intervals that define the structure of trapezoid shown in Figure 3. The lower limit is in $[I_{min}, I_{mid1}]$ as shown in Figure 4 (interval A) and the upper limit is in in $[I_{mid2}, I_{max}]$ as shown in Figure 5 (interval C). The interval B defined as $[I_{mid1}, I_{mid2}]$ is flat 1 as shown in Figure 3.

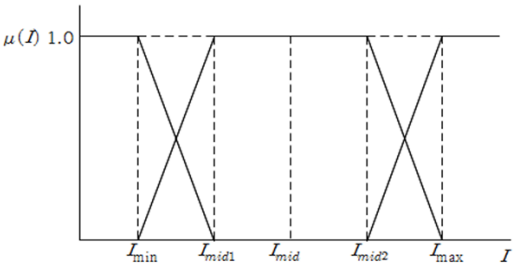

Figure 3. Membership function for fuzzy stretching

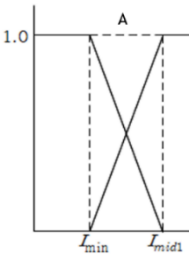

Figure 4. Membership for lower limit

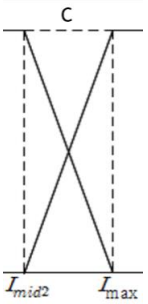

Figure 5. Membership for upper limit

With center-of-gravity method, the defuzzification process is defined as equation (6), (7), (8) where α, β denote the lower and upper limit in fuzzy stretching respectively.

$$\alpha = \frac{\sum_{i=0}^{mid} u(I_i) I_i}{\sum_{i=0}^{mid} u(I_i)} \tag{6}$$

$$\beta = \frac{\sum_{j=mid}^{max} u(I_j) I_j}{\sum_{j=mid}^{max} u(I_j)} \tag{7}$$

$$f(I) = \frac{I-\alpha}{\beta-\alpha} \tag{8}$$

where f(I) is the stretched intensity value of current pixel I. The effect of proposed fuzzy stretching is as shown in Figure 6.

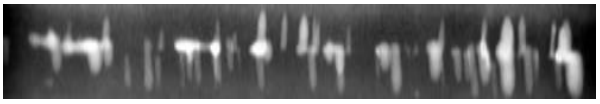

Figure 6. The effect of fuzzy stretching

B. Defect detection with fcm based fuzzy binarization

In the binarization process, it is important to have critical threshold value relatively immune to its environment. Especially for ceramic welding defect detection, defects appear in various ways such that any method with fixed threshold often fails to obtain proper result (Silveria *et al.*, 2009; Kim & Woo, 2014; Kim & Song, 2016). In this paper, we apply fuzzy binarization. In that process, the binarization is only applied to pixels having relatively higher membership degree with respect to a threshold called α-cut (Kim *et al.*, 2014). We propose a method to define such threshold as a function of the Fuzzy C-Means clustering that has been successfully used in medical imaging application (Kim *et al.*, 2018). FCM is used to determine binarization threshold α-cut as shown in Figure 7 and equation (12).

The FCM process in this paper is as following;

Step 1: Initialize c (2≤c<n) and exponential weight m (1≤m<∞). Also initialize the error threshold (ε) for terminating condition and the membership degree U(0).

Step 2: Compute the value of central vector v_{ij} as shown in equation (9) for $\{v_i \mid i=1, 2, \ldots, c\}$.

$$v_{ij} = \frac{\sum_{k=1}^{n}(U_{ik})^m x_{kj}}{\sum_{k=1}^{n}(U_{ik})^m} \tag{9}$$

where X is the input pattern, *i* is the cluster index, *j* is the pattern node index. *k* is the pattern index, *n*is the number of patterns, and *U* is the membership function.

Step 3: Define the distance metric as equation (10).

$$d_{ik} = \sqrt{\sum_{j=1}^{l}(x_{kj} - v_{ij})^2} \tag{10}$$

where the distance d_{ik} is defined as between the k-th pattern x_k and the central vector of the *i*-th cluster, and u_{ik} is the membership degree of x_k among patterns in the *i*-th cluster.

The new membership degree function $U^{(r+1)}$ is defined as equation (11).

$$U^{(r+1)} = 1/\sum_{j=1}^{c}(\frac{d^r{}_{ik}}{d^r{}_{jk}})^2, \text{for } I_k = \emptyset \tag{11}$$

where l denotes the number of pattern nodes and c denotes the number of clusters.

Step 4: Compute the difference ($U^{(r+1)}$-$U^{(r)}$) between the new membership and the previous membership degree. If the difference is less than the error threshold (ε), then the algorithm terminates otherwise go to Step 2.

Obtained intensity values of cluster centers are then applied to equation (12).

$$\alpha - cut = \frac{\sum_{j=1}^{c}\eta_i}{c}/255 \tag{12}$$

where c denotes the number of clusters and η denotes the cluster centre pixel.

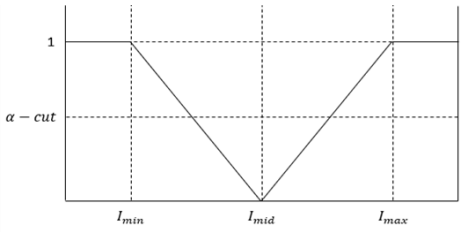

Figure 7. Membership function for fuzzy binarization

Critical interval defining points [I_{min} , I_{mid} , I_{max}] are computed as equation (4) of fuzzy stretching process. Then the final binarization us done with equation (13). The effect of fuzzy binarization is shown as Figure 8.

$$\begin{aligned} &if(X_m < I_{min})\ \mu(y) = 1 \\ &else\ if(X_m > I_{min}\ and\ X_m < I_{mid})\ \mu(y) = \frac{X_m - I_{min}}{I_{mid} - I_{min}} \\ &else\ if(X_m > I_{mid})\ \mu(y) = 0 \end{aligned} \tag{13}$$

Figure 8. The effect of proposed fuzzy binarization

III. RESULT AND DISCUSSION

The proposed method is implemented with Microsoft Visual Studio 2017 on the IBM-compatible PC Intel(R) Core(TM) i5-8400 CPU with 8.0 GB RAM. Welding X-ray images are from NDT and Radiation Safety Center at Dong-Eui University, Pusan, Korea. Total 80 images for defect detection testing of ship building ceramic materials with various thicknesses - 8mm, 10mm, 11mm, 16mm, and 22mm. Various detection results with different thickness are shown in Figure 9.

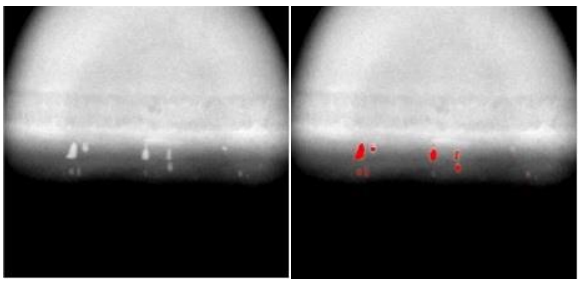

(a) 8mm Case Defect Detection

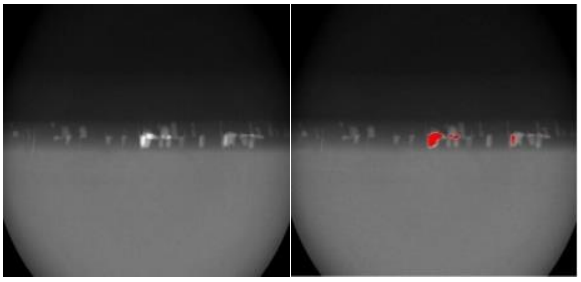

(b) 10mm Case Defect Detection

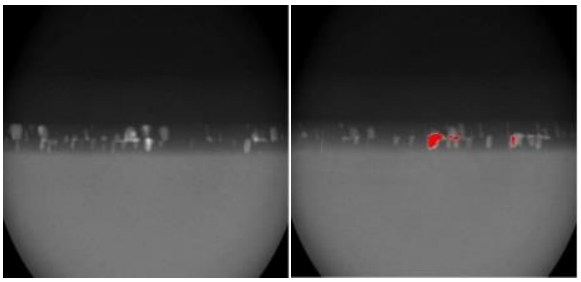

(c) 11mm Case Defect Detection

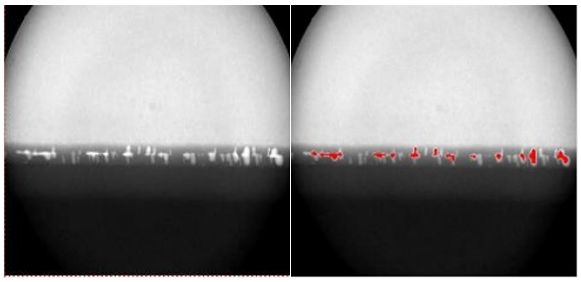

(d) 16mm Case Defect Detection

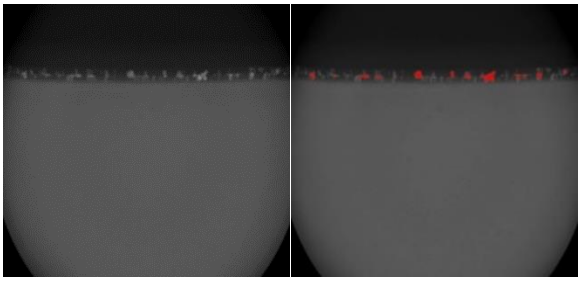

(e) 22mm Case Defect Detection

Figure 9. Automatic defect detection examples

In Figure 9, for each thickness value case, detected defect is represented in red at the image below the input.

The performance of proposed method is compared with K-means based approach (Kim & Woo, 2014) as summarized in Table 1. In that K-means based approach, Max-Min binarization was used. That strategy was cheap and easy to understand but the performance was unsatisfactory since K-means could not discriminate defected pixels from normal area with low contrasted images. A typical example that the proposed method overcomes the failure of K-means based approach is shown in Figure 10.

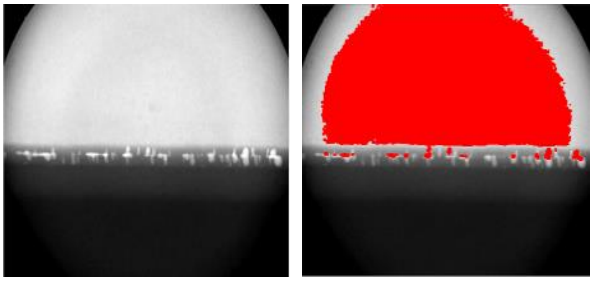

(a) Input (b) Failed by K-means

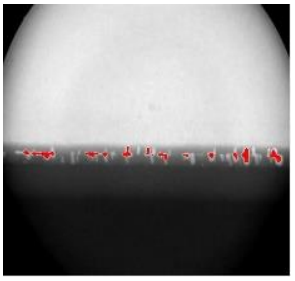

(c) Defect Detection by Proposed Method

Figure 10. Comparison of proposed method with K-means based method

Table 1. Defect detection performance result

Thickness	K-Means	Proposed	Total
8mm	0	13	15
10mm	16	19	20
11mm	9	10	10
16mm	0	8	10
22mm	18	24	25
Total	43	74	80
Success	53.8%	92.5%	

The performance of defect detection is improved remarkably as shown in Table 1. Although fuzzy stretching - FCM - Fuzzy binarization procedure proposed in this paper is computationally more expensive than the simple K-means with Min-Max binarization approach (Kim & Woo, 2014), it is worth doing in that the performance of the proposed method is much better and more stable. The proposed method successfully detect welding defects in between 80% and 100% regardless of the thickness of given images whereas K-means based approach totally fails to find defects in 8mm and 16mm data.

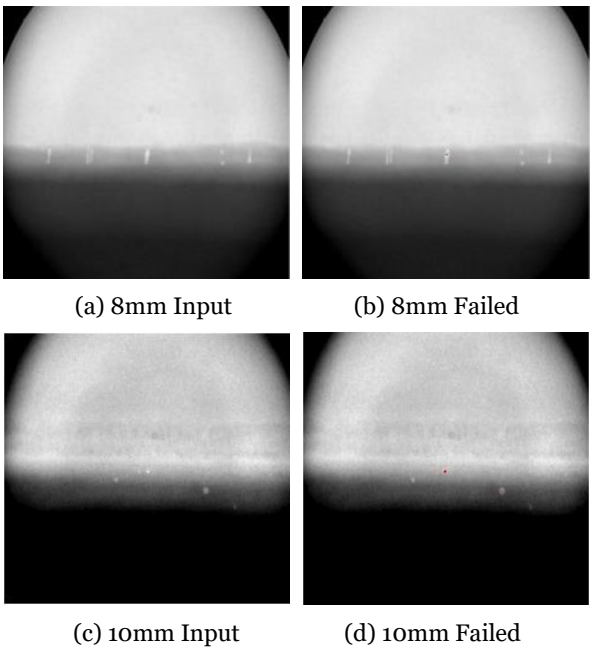

(a) 8mm Input (b) 8mm Failed

(c) 10mm Input (d) 10mm Failed

Figure 11. Failed defect detection

Unfortunately, the proposed method still fails to detect defects in some cases as shown in Figure 11. With our post-hoc analysis, we find that the proposed method may have over- or under-estimate the cluster centre intensities in FCM process in failed cases. Specifically, there exists a trend to have extremely skewed distributions of centre points in FCM. Thus, the critical threshold is not appropriately given. We doubt that the fixed initialization of the number of clusters in FCM process is the reason of such failure.

IV. CONCLUSION

In this paper, we propose a fuzzy logic based automatic segmentation approach to detect welding defects of various thickness cases from X-rayed images. Initial noise reduction is done with anisotropic filtering that has no aliasing effect. Image intensity contrast is enhanced by least square method and fuzzy stretching. Then, we apply fuzzy binarization with environment adaptive threshold based on FCM clustering. Membership functions for these fuzzy control is given trapezoid type thus interval control should be carefully treated in this approach.

In experiment with 80 images of five different thickness cases, the proposed method shows 92.5% success in defect detection that is a remarkable improvement from previous K-means based approach. Also, there was no more than 2 cases of the same thickness (among 10 ~ 25 input images for each thickness type) of failed defect detection.

From a post-hoc analysis of a few failed cases of this experiment, we doubt that the fixed number of clusters may cause FCM process less flexible than expected and that is the main source of a few failed cases of this experiment. We may need to explore a dynamic control strategy for FCM or a deep learning approach that arises very recently in this field (Ferguson *et al.*, 2018) to avoid such failure.

V. REFERENCES

Abdallah, MB, Malek, J, Azar, AT, Belmabrouk, H, Monreal, JE & Krissian, K 2016, Adaptive noise-reducing anisotropic diffusion filter, '*Neural Computing and Applications*', vol. 27, no. 5, pp.1273-1300.

Chao, SM & Tsai, DM 2006, 'Astronomical image restoration using an improved anisotropic diffusion', *Pattern Recognition Letters*, vol. 27, no. 5, pp.335-344.

Chen, S, Lin, B, Han, X & Liang, X 2013, 'Automated inspection of engineering ceramic grinding surface damage based on image recognition', *The International Journal of Advanced Manufacturing Technology*, vol. 66, issue. 1-4, pp.431-443.

Ferguson, M, Ak, R, Lee, YTT & Law, KH 2018, 'Detection and Segmentation of Manufacturing Defects with Convolutional Neural Networks and Transfer Learning', *arXiv preprint* arXiv:1808.02518.

Grazzini, J, Turiel, A & Yahia, H 2005, 'Presegmentation of high-resolution satellite images with a multifractal reconstruction scheme based on an entropy criterium', In *IEEE International Conference on Image Processing 2005*, vol. 1, pp. I-649.

Hocenski, Z, Vasilic, S & Hocenski, V 2006, 'Improved canny edge detector in ceramic tiles defect detection', In *IECON 2006-32nd Annual Conference on IEEE Industrial Electronics*, pp. 3328-3331.

Kahanov, Y, Ashkenazi, D, Cvikel, D, Klein, S, Navri, R & Stern, A 2015, 'Archaeometallurgical analysis of metal remains from the Dor 2006 shipwreck: a clue to the understanding of the transition in ship construction', *Journal of Archaeological Science: Reports*, no. 2, pp.321-332.

Kesharaju, M, Nagarajah, R, Zhang, T & Crouch, I 2014, 'Ultrasonic sensor based defect detection and characterisation

of ceramics', *Ultrasonics*, vol. 54, no. 1, pp.312-317.

Kim, KB & Song, DH 2016, 'An Advanced Ceramic Defect Detection with Anisotropic Filtering and Diagonal Binarization', *International Information Institute (Tokyo) Information*, vol. 19, no. 1, pp. 181-189.

Kim, KB & Song, DH 2017, 'Automatic Defect Detection using Fuzzy Binarization and Brightness Contrast Stretching from Ceramic Images for Non-Destructive Testing', *Journal of Korea Institute of Information and Communication Engineering*, vol. 21, no. 11, pp. 2121-2127.

Kim, KB & Woo, YW 2010, 'Detection of Flaws in Ceramic Materials Using Non-Destructive Testing', *The Journal of the Korea institute of electronic communication sciences*, vol. 5, no. 3, pp.321-326.

Kim, KB & Woo, YW 2014, 'Fault Detection of Ceramic Imaging using K-means Algorithm', In *Proceedings of Conference of Korea Society of Computer Information*, vol. 22, no.1, pp. 275-277.

Kim, KB, Song, DH & Lee, WJ 2014, 'Flaw detection in ceramics using sigma fuzzy binarization and gaussian filtering method', *International Journal of Multimedia and Ubiquitous Engineering*, vol. 9, no. 1, pp.403-414.

Kim, KB., Song, DH & Yun, SS 2018, 'Automatic Extraction of Blood Flow Area in Brachial Artery for Suspicious Hypertension Patients from Color Doppler Sonography with Fuzzy C-Means Clustering', *Journal of information and communication convergence engineering*, vol. 16, no. 4, pp.258-263.

Ma, BQ & Zhou, ZG 2014, 'Progress and development trends of composite structure evaluation using noncontact nondestructive testing techniques in aviation and aerospace industries', *Acta Aeronautica et Astronautica Sinica*, vol. 35, no. 7, pp.1787-1803.

Mansoory, MS, Tajik, H, Mohamadi, G & Pashna, M 2008, 'Edge defect detection in ceramic tile based on boundary analysis using fuzzy thresholding and radon transform', *In 2008 IEEE International Symposium on Signal Processing and Information Technology*, pp. 58-62.

Marefat, F, Faghedi, MR, Khodabandeh, AR & Reza, M 2011, 'Capabilities and Limitations of Radiography and Phased Array Ultrasonic Test in the Detection of subtle welding defects', In *Singapore international NDT conference & exhibition*.

Meihua, X & Zhengming, W 2004, 'Fingerprint enhancement based on edge-directed diffusion', In *Third International Conference on Image and Graphics (ICIG'04)*, pp. 274-277.

Perona, P & Malik, J 1990, 'Scale-space and edge detection using anisotropic diffusion', *IEEE Transactions on Pattern Analysis and Machine Intelligence*, vol. 12, no. 7, pp.629–639.

Rajkolhe, R & Khan, JG 2014, 'Defects, causes and their remedies in casting process: A review', *International Journal of Research in Advent Technology*, vol. 2, no. 3, pp.375-383.

Sarin, CR, Karthik, M, Anilesh, M & Subramaniam, P 2012, 'Advanced Image Enhancement of Ultrasonic Scan Images For Intelligent Quality Inspection of Adhesively Bonded Joints in Ceramics', *International Journal of Advanced Research in Computer Science and Software Engineering*, vol. 2, no. 4, pp.302-306.

Shin, CH & Jung, CY 2017, 'An Optimal Algorithm for Enhancing the Contrast of Chest Images Using the Frequency Filters Based on Fuzzy Logic', *Journal of information and communication convergence engineering*, vol. 15, no. 2, pp.131-136.

Silveira, J, Ferreira, MJO, Santos, C & Martins, T 2009, 'Computer vision techniques applied to the quality control of ceramic plates', In *IEEE International Conference on Industrial Technology (ICIT 2009)*.

Suratkar, A, Sajjadi, AY & Mitra, K 2013, 'Non-destructive evaluation (NDE) of composites for marine structures: detecting flaws using infrared thermography (IRT)', In *Non-Destructive Evaluation (NDE) of Polymer Matrix Composites, Woodhead Publishing*, pp. 649-668e.

Thiruganam, M, Anouncia, SM & Kantipudi, S 2010, 'Automatic defect detection and counting in radiographic weldment images', *International Journal of Computer Applications*, vol. 10, no. 2, pp.1-5.

Valavanis, I & Kosmopoulos, D 2010, 'Multiclass defect detection and classification in weld radiographic images using geometric and texture features', *Expert Systems with Applications*, vol. 37, no. 12, pp.7606-7614.

Villain, N, Goussard, Y, Idier, J & Allain, M 2003, 'Three-dimensional edge-preserving image enhancement for computed tomography', *IEEE transactions on Medical Imaging*, vol. 22, no. 10, pp.1275-1287.

Wang, G & Liao, TW 2002, 'Automatic identification of different types of welding defects in radiographic images', *Ndt & E International*, vol. 35, no. 8, pp.519-528.

Zapata, J, Vilar, R & Ruiz, R 2010, 'An adaptive-network-based fuzzy inference system for classification of welding defects', *NDT & e International*, vol. 43, no. 3, pp.191-199.

Zhang, W 2016, 'Technical problem identification for the failures of the liberty ships', *Challenges*, vol. 7, no. 2, p.20.